



PERGAMON

Journal of South American Earth Sciences 15 (2003) 731–748

Journal of
**South American
Earth Sciences**

www.elsevier.com/locate/jsames

Orogenic shortening and the origin of the Patagonian orocline (56° S.Lat)

Pablo E. Kraemer*

Pecom Energia S.A., J.J. Lastra 6000 (8300) Neuquén, Argentina

Received 1 August 2002; accepted 1 September 2002

Abstract

A maximum shortening of 600 km and a minimum of 300 km was calculated for the southernmost extreme of the Patagonian Andes orocline. A regional balanced cross-section was restored in four stages that represent the main events of compressive deformation. The mid-Cretaceous event produced a maximum shortening of 430 km associated with high grade regional metamorphism in Cordillera Darwin and a period of fast subsidence in the Magallanes foreland basin during the Late Cretaceous. The Late Cretaceous–Cenozoic events produced a maximum shortening of 170 km, of which 40 km correspond to Late Cretaceous, 50 km to Paleogene, and 80 km to Neogene events. A set of evolutive profiles at lithospheric scale from Jurassic to Present time shows that, assuming a maximum shortening of 600 km, the mass balance is attained only if the back arc oceanic lithosphere created during the early rifting stage is partially consumed by a short episode of reverse subduction during the mid-Cretaceous compressive event. A set of six maps showing the palinspastic restoration of the Patagonian Andes orocline indicates that a maximum shortening of 600 km at the southern extreme is compatible with the available geologic data and geometrically compatible with paleomagnetic arc rotations of nearly 90°.

© 2002 Elsevier Science Ltd. All rights reserved.

Keywords: Patagonian andes orocline; Fold belt; Shortening; Cretaceous

Resumen

Se calculó un acortamiento orogénico máximo de 600 km y mínimo de 300 km para el extremo sur del orocline de los Andes Patagónicos. Una sección regional balanceada fue restituida en cuatro etapas representando los eventos compresivos principales. En el evento Cretácico medio se habría producido un acortamiento máximo de 430 km asociado a metamorfismo regional de alto grado en la cordillera Darwin y un período de rápida subsidencia en la cuenca de antepaís de Magallanes. Los eventos compresivos del Cretácico Tardío y el Cenozoico habrían producido un acortamiento máximo de 170 km, distribuidos en 40 km durante el cretácico tardío, 50 km en el Paleógeno y 80 km en el Neógeno. Una serie de perfiles a escala litosférica abarcando del Jurásico al presente muestran que asumiendo valores de acortamiento máximos de 600 km, el balance de masas es posible sólo si se admite un rápido episodio de subducción reversa en el Cretácico medio, en el que se habría consumido parte de la litósfera oceánica de trasarco creada durante el estadio de rifting inicial. Se realizaron seis mapas palinspásticos del orocline Patagónico mostrando que el acortamiento orogénico máximo calculado de 600 km es compatible con la evolución geológica regional y consistente con las rotaciones de hasta 90° obtenidas de estudios paleomagnéticos.

© 2002 Elsevier Science Ltd. All rights reserved.

1. Introduction

The Patagonian Andes orocline is located along the arcuate active margin of southernmost South America (Fig. 1). Some prominent features of this region south of 50°S are the progressive southward bending of the mountain range, a belt of basic rocks in the back arc region, and a unique Mesozoic high grade metamorphic core (Nelson

et al., 1980; Dalziel, 1981; Dalziel and Brown, 1989; Kohn et al., 1995).

The amount of orogenic shortening provides useful information to generate paleogeographic maps that show the past positions of the magmatic arc, fold belt, and back arc basin relative to the stable foreland during the evolution of the orocline. Local shortening estimations were performed at the frontal fold belt (Winslow, 1981; Alvarez Marrón et al., 1993) and at regional scale (Mingramm, 1982) with values varying between 30 and 160 km, respectively.

* Fax: +54-299-449-1361.

E-mail address: pkraemer@pecom.com (P.E. Kraemer).

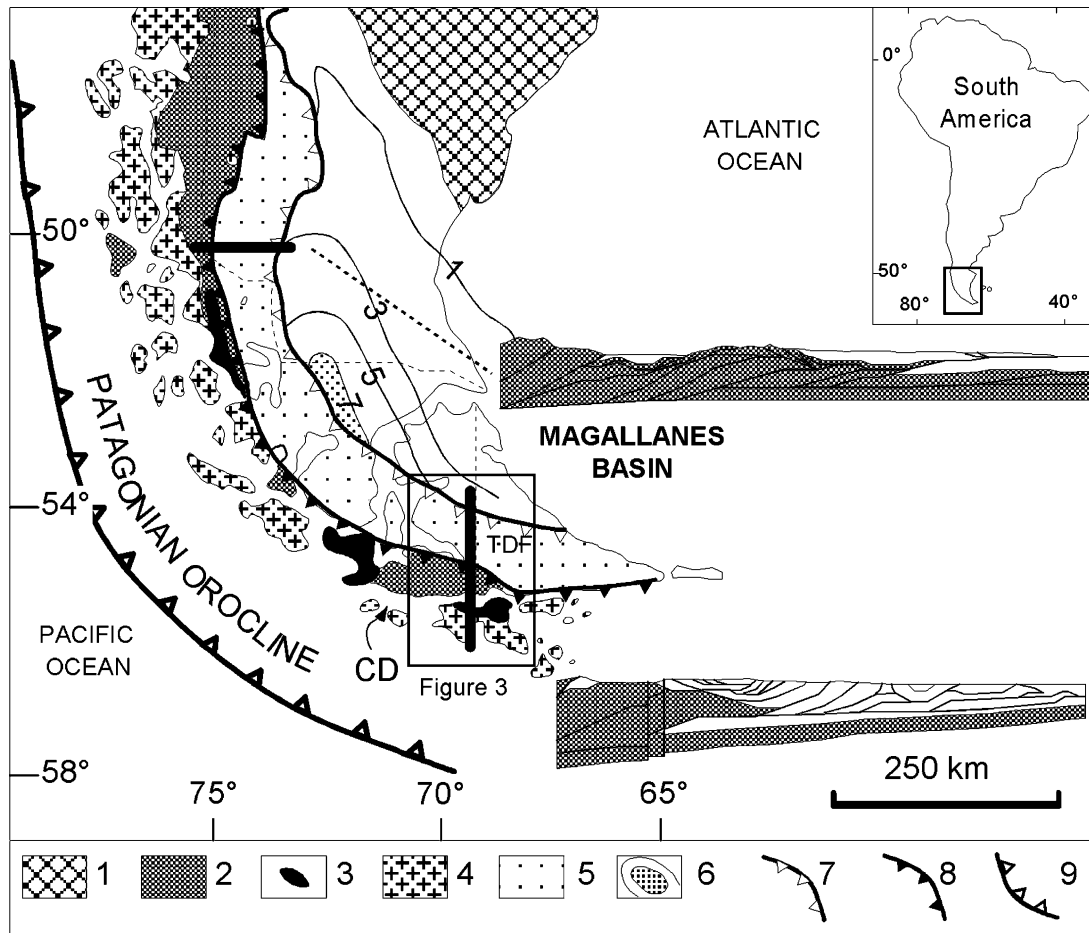


Fig. 1. Map of the Patagonian orocline showing the main geologic regions. Solid bars show the location of two regional cross-sections used to estimate the orogenic shortening (Kraemer, 1996, 1998). CD: Cordillera Darwin metamorphic core, TDF: isla de Tierra del Fuego. 1: Deseado massif, 2: basement thrust zone, 3: Upper Jurassic–Lower Cretaceous basic rocks, 4: Mesozoic–Cenozoic Patagonian batholith, 5: foreland fold belt, 6: contour lines of sedimentary infill (km), 7: fold belt front; 8: basement thrust zone front, 9: subduction zone.

The structural complexity of the fold belt (Cagnolatti et al., 1987; Alvarez Marrón et al., 1993; Klepeis, 1994), estimations of 25 km of crustal thickening in the metamorphic core of Cordillera Darwin (Nelson, 1982; Kohn et al., 1995), and rotations of 90° in the magmatic arc (Cunningham et al., 1991) strongly suggest that the Patagonian orocline underwent a much more intense total contraction than was previously estimated.

The main goal of this paper is to reexamine the amount of Mesozoic–Cenozoic orogenic shortening of the Patagonian Andes of Tierra del Fuego. To achieve this goal, all available geologic data (Caminos, 1980; Nelson et al., 1980; Caminos et al., 1981; Mingramm, 1982; Nelson, 1982; Suarez et al., 1985; Cagnolatti et al., 1987; Alvarez Marrón et al., 1993; Klepeis, 1994; Kohn et al., 1995; Klepeis and Austin, 1997) were compiled for a north–south transect, and a regional balanced cross-section was restored in four stages from mid-Cretaceous to Late Cenozoic time. The uncertainty in the calculation of shortening increases from the less deformed and better constrained fold belt to the highly deformed and metamorphosed internal zone of the orogen. This is reflected in the spread of the total shortening

estimations, which range from a maximum of 600 km to a minimum of 300 km and are several times larger than previous estimations.

To test and discuss the results, a set of profiles at lithospheric scale and five palinspastic maps from the Jurassic to the Present time were constructed assuming a maximum value of shortening. This analysis shows that the mass balance is attained only if part of the oceanic lithosphere created at the back arc early rifting stage was consumed by a short-lived, arc-directed subduction during the mid-Cretaceous. The palinspastic restoration of the Patagonian Andes orocline shows that a maximum total shortening of 600 km is geologically reasonable and can explain the magmatic arc rotations of nearly 90° obtained from paleomagnetic studies.

2. Geologic setting

Three main geologic regions are recognized at the southern tip of South America: the Patagonian Andes orocline along the active margin, the Magallanes basin, and

the Deseado massif, a block of upper Proterozoic–Paleozoic basement at the northeastern edge of the basin (Fig. 1).

The western Patagonian Andes expose a 1500 km arcuate belt of Mesozoic–Cenozoic plutonic rocks of the Patagonian batholith (Halpern, 1973; Nelson et al., 1988). Only sparse Upper Paleozoic–Lower Mesozoic rocks crop out along the Pacific coast (Forsythe and Mpodozis, 1979), but a semicontinuous belt of sedimentary and metamorphic basement rocks extends along the eastern margin of the batholith (Hervé et al., 1981b). This belt of Paleozoic rocks, or basement thrust zone (Kraemer, 1998), roughly coincides with the highest Andean topography (Fig. 1).

South of 50°S, basic rocks with oceanic affinities of the Sarmiento and Tortuga complexes are interpreted as deformed oceanic crust of a Mesozoic marginal basin (Dalziel and Cortés, 1972; Katz, 1972; Bruhn, 1979; Allen, 1982).

The Magallanes basin, located between the Patagonian Andes and the Deseado massif, is filled by more than 7 km of Upper Jurassic–Cretaceous and Tertiary marine and continental deposits (Russo et al., 1980).

3. Geologic evolution

The basin evolution broadly consists of an initial extensional stage followed by a foreland or compressive stage (Biddle et al., 1986) (Fig. 2).

The initial extensional stage was associated with Middle–Late Jurassic regional silicic volcanism (Bruhn, 1979) and continental and marine sedimentation associated with normal faulting (Uliana et al., 1985). During this stage, oceanic crust was created in the back arc basin, a transgressive megasequence was deposited, and the marine deposits reached their maximum north and northeast extension (Riccardi and Rolleri, 1980; Aguirre Urreta and Ramos, 1981; Biddle et al., 1986; Aguirre Urreta, 1990). During the foreland stage, the basin was affected by several pulses of compressive deformation and filled by a complex Late Cretaceous–Tertiary regressive megasequence (Natlund et al., 1974; Arbe and Hechem, 1984; Biddle et al., 1986; Wilson, 1991).

The oldest unit recognized is a sedimentary metamorphic basement of Late Paleozoic–Early Mesozoic age (Caminos et al., 1981; Hervé et al., 1981a,b) that crops out in the metamorphic core of Cordillera Darwin (Klepeis, 1994; Kohn et al., 1995; Nelson, 1982) (Fig. 3).

Plutonic bodies of tonalites, granites, granodiorites, diorites, and gabbros of the Patagonian batholith, interpreted as exposed roots of a Middle Jurassic–Neogene magmatic, crop out along the Pacific coast and shores of the Beagle Channel (Halpern, 1973; Ramos et al., 1982; Nelson et al., 1988) (Fig. 3).

The basement is unconformably covered by Middle–Upper Jurassic acidic volcanics and volcanoclastic rocks of

the Tobífera Formation (Bruhn et al., 1978). This unit has wide subsurface distribution in the Magallanes basin with frequent changes in thickness in local grabens (Uliana et al., 1985; Klepeis and Austin, 1997) and crops out along the transect at the north and south slopes of Cordillera Darwin (Fig. 3).

The Tobífera is unconformably covered by Upper Jurassic–Lower Cretaceous littoral to continental sandstones and platform shales (Riccardi and Rolleri, 1980; Wilson, 1991). In Tierra del Fuego, the platform shales of the Magallanes basin are replaced laterally by slope deposits and deep ocean turbidites of the Yaghan Formation, with increasing participation of volcanic and volcanoclastic facies toward the south (Suarez and Pettigrew, 1976; Winn, 1978; Caminos et al., 1981; Klepeis, 1994) (Fig. 2(A)). These rocks crop out extensively along the shores of the lago Fagnano, Seno Almirantazgo, and Beagle Channel (Fig. 3).

South of the Beagle Channel there are abundant outcrops of Upper Jurassic–Lower Cretaceous pillow lavas, sheeted dikes, and gabbros of the Tortuga complex covered by volcanoclastic rocks (Fig. 3). The Tortuga complex is an incomplete ophiolitic sequence composed of pillow lavas, sheeted dikes, and gabbros that represent upper levels of the oceanic crust formed in the back arc basin (Suarez and Pettigrew, 1976; Suarez et al., 1985).

The Tortuga complex is interpreted as the remnant oceanic floor of a marginal basin opened during the Late Jurassic–Early Cretaceous (Dalziel and Cortés, 1972; Katz, 1972; Suarez and Pettigrew, 1976) and filled with volcanoclastic turbidites sourced in an active calc-alkaline volcanic arc (Suarez and Pettigrew, 1976; Winn, 1978; Suarez, 1979; Suarez et al., 1985) (Fig. 2(A)). The metamorphism and geochemistry of these rocks support an origin related to a spreading center (Saunders et al., 1979; Stern and Elthon, 1979), but ultrabasic rocks were not found in either the Tortuga complex or the Sarmiento complex toward the north (Allen, 1982).

At the end of the Lower Cretaceous, deep ocean turbidites of Aptian–Albian age were deposited (Katz, 1963; Scott, 1966; Wilson, 1991), as well as sediments with a clear western source (Aguirre Urreta and Ramos, 1981; Arbe and Hechem, 1984; Aguirre Urreta, 1990).

The Jurassic–Lower Cretaceous stratigraphic units, deposited during the extensional stage in platform-slope, deep ocean, and magmatic arc environments, are gathered into the tectostratigraphic unit S1, which is bounded at its top by the mid-Cretaceous unconformity (Fig. 2(A)).

The compressional or foreland stage (Fig. 2(B)) begins with the initial deformation of the western and southwestern margin of the basin during mid-Cretaceous time and extends until the latest pulses of deformation during Neogene time.

The mid-Cretaceous event, which is the lower boundary of the tectostratigraphic unit S2, is a regional Albian–Cenomanian unconformity. It is recognized in the subsurface (Biddle et al., 1986) and the surface (Arbe, 1989) and

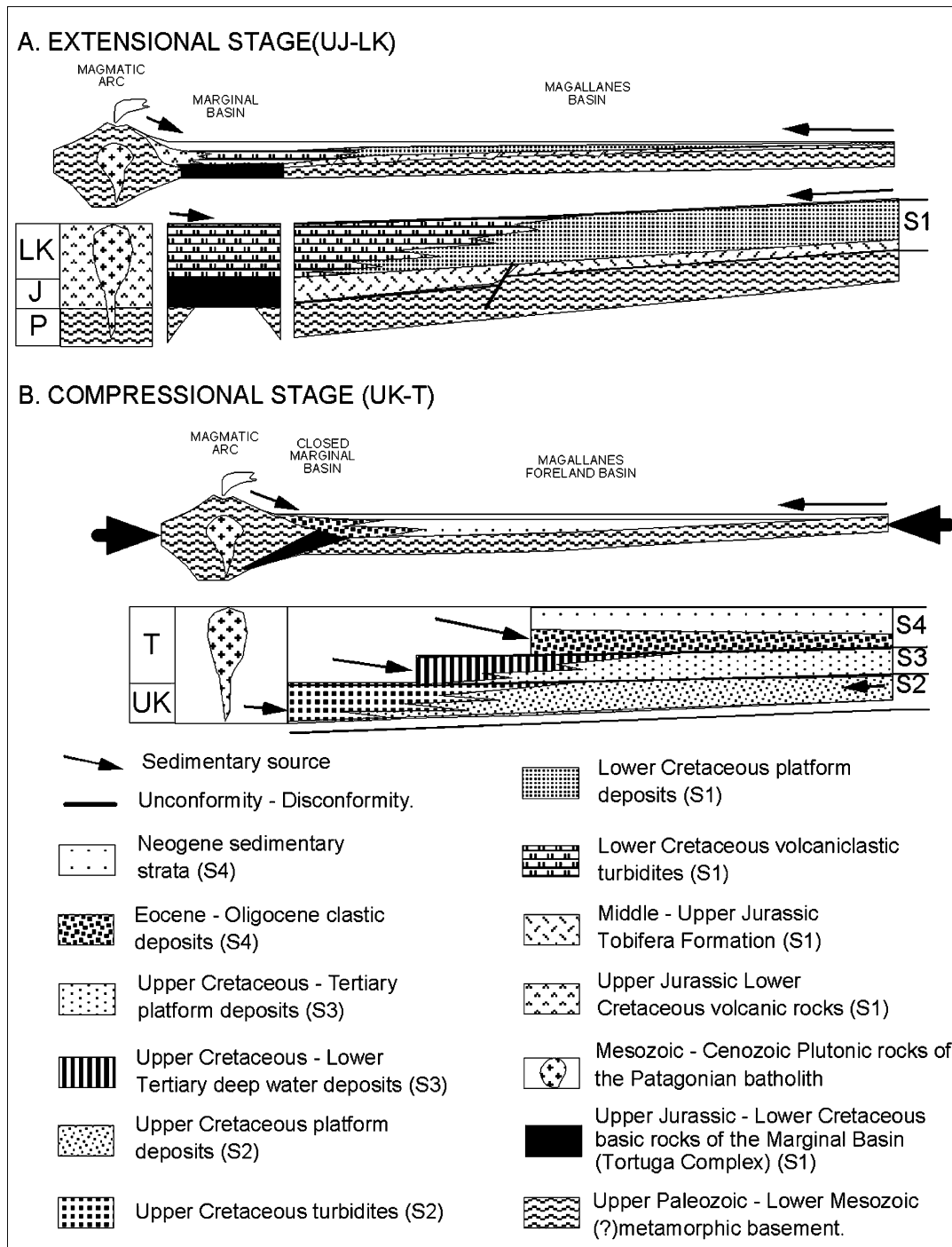


Fig. 2. Tectostratigraphic evolution of the Patagonian Andes of Tierra del Fuego. During the extensional stage (A), the three main tectonic environments were the Magallanes basin, the marginal basin, and the magmatic arc. The rocks deposited during this stage are gathered in the tectostratigraphic unit S1. During the compressional stage (B), the main tectonic environments were the Magallanes foreland basin and the magmatic arc. The rocks deposited during the different compressive events are separated into three tectostratigraphic units: S2, S3, and S4.

related to a deformational event between 87–90 and 100–110 Ma in the islands south of the Beagle Channel (Halpern and Rex, 1972).

The mid-Cretaceous deformation is related to a period of increasing velocity of plate convergence, which transported the magmatic arc toward the continent, closed the back arc marginal basin (Dalziel et al., 1974; Dalziel and Palmer,

1979) (Fig. 2(B)), and deformed and metamorphosed the continental transitional crust of the Magallanes basin, as represented by the basement core of Cordillera Darwin (Bruhn, 1979) (Fig. 3).

The basement rocks of Cordillera Darwin record an episode of foreland vergent folding, foliation, and thrusting [D1] followed by hinterland vergent folding and foliation

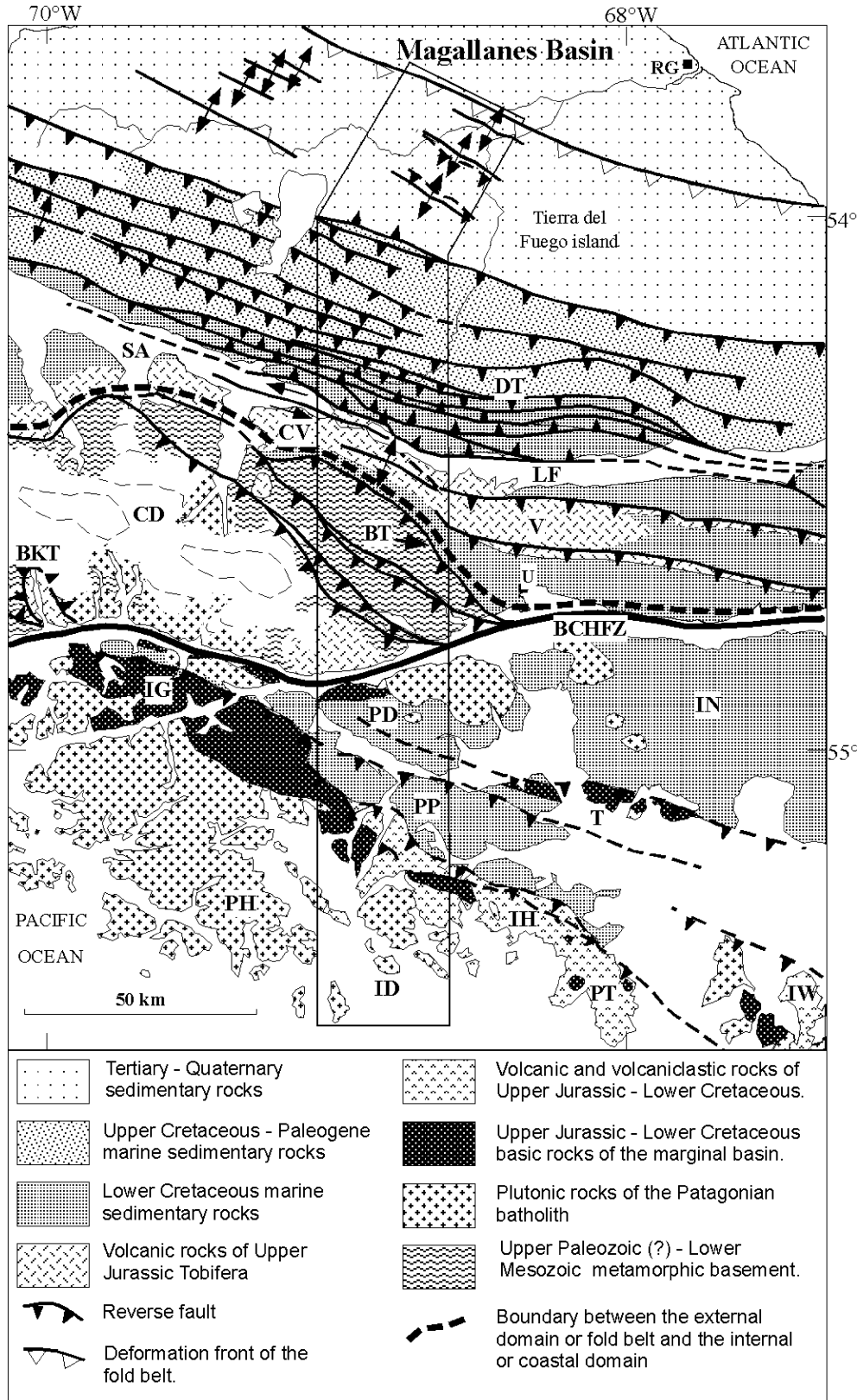


Fig. 3. Geologic map of the Patagonian Andes compiled from Alvarez Marrón et al. (1993), Cagnolatti et al. (1987), Caminos (1980), Klepeis (1994), Mingramm (1982), Nelson (1982), and Suarez et al. (1985). See Fig. 1 for location. RG: Rio Grande, DT: Deseado thrust, SA: Seno Almirantazgo, CV: Cerro Verde anticline, LF: lago Fagnano, V: Sierra de Valdivieso, BT: basement thrust, CD: Cordillera Darwin, BKT: backthrust, U: Ushuaia, BCHFZ: Beagle Channel fault zone, PD: península Dumas, IG: isla Gordon, IN: isla Navarino, PP: península Pasteur, ID: isla Duperre, IH: isla Hoste, PH: península Hardy, IW: isla Wollaston, PT: península Tekenika. The open rectangle shows the location of the regional section of Fig. 5.

[D2] synchronous with a metamorphic peak at 90 Ma and a period of rapid exhumation and cooling between 90–70 Ma (Nelson et al., 1980; Kohn et al., 1995). The rapid exhumation in Cordillera Darwin coincides with an episode of fast subsidence and deposition of deep ocean turbidites in the foreland basin (Natland et al., 1974; Biddle et al., 1986). During this stage, the subsidence rate increased dramatically and the basin began to receive detritus from a western–southwestern active orogenic source during Cenomanian times. Deep ocean turbidites with a northwest precedence (Katz, 1963; Scott, 1966; Arbe and Hechem, 1984; Wilson, 1991) were deposited at the northern part of the basin.

In Tierra del Fuego, a continuous belt of Upper Cretaceous deep ocean turbidites (Caminos, 1980; Alvarez Marrón et al., 1993) crops out north of Cordillera Darwin (Fig. 3).

These turbidite deposits pinch out laterally to fine-grained clastic platform deposits toward the north and east (Caminos, 1980; Russo et al., 1980; Biddle et al., 1986; Mingramm, 1982; Alvarez Marrón et al., 1993). The turbidites are covered by Late Cretaceous platform deposits (Caminos, 1980; Olivero and Malumian, 1999).

The Upper Cretaceous turbidites and platform deposits are gathered in the tectostratigraphic unit S2 (Fig. 2), which is bounded at its top by a regional late Maastrichtian–early Paleocene angular unconformity (Caminos, 1980).

This unconformity was identified in the subsurface in Tierra del Fuego (Biddle et al., 1986; Alvarez Marrón et al., 1993) and as a surface angular unconformity between the Campanian–Maastrichtian and late Paleocene–Eocene (Caminos, 1980; Olivero and Malumian, 1999). The same unconformity, related to an episode of Andean uplift and changes in the rock type at the western source area, was described further north (Macellari et al., 1989).

This unconformity is associated with a renewed deepening of the basin. The subsurface thickness patterns suggest an Andean source for the Paleogene formations (Biddle et al., 1986). In Tierra del Fuego, the Paleogene formations crop out in a continuous belt parallel to the Seno Almirantazgo and lago Fagnano (Fig. 3). The stratigraphic units deposited at this time include turbidites (Alvarez Marrón et al., 1993) and platform deposits (Caminos, 1980; Biddle et al., 1986; Olivero and Malumian, 1999). These formations are grouped in the tectostratigraphic unit S3 (Fig. 2(B)).

The upper boundary of S3 in Tierra del Fuego is the angular unconformity at the base of upper Eocene–lower Oligocene fan delta conglomerates with clear Andean provenances (Biddle et al., 1986; Malumian and Nañez, 1988; Olivero and Malumian, 1999) (Fig. 2). This unconformity is related to a deformation event and a pulse of rapid exhumation and cooling between 60 and 40 Ma (late Paleocene–early to middle Eocene) in Cordillera Darwin (Nelson, 1982; Kohn et al., 1995). The Eocene–lower Oligocene clastics are covered by marine and

continental deposits of Oligocene–Miocene age (Thomas, 1949; Alvarez Marrón et al., 1993).

The Eocene–Oligocene–Miocene formations crop out along the frontal fold belt north of Seno Almirantazgo and lago Fagnano and are gathered in the tectostratigraphic unit S4, which is unconformably covered by glaciofluvial deposits of Pliocene–Pleistocene age (Fig. 3).

The Neogene angular unconformity, which is the upper boundary of S4, is located at the base of glaciofluvial deposits of Pliocene–Pleistocene age. This unconformity is related to a deformation event recognized in seismic lines along the Magallanes strait (Yañez et al., 1988) and Diego Ramirez basin south of Hardy peninsula (González, 1989) (Fig. 4(A) and (C)). North of 50°S, a late Miocene episode of deformation was described in the fold belt (Ramos, 1989; Kraemer, 1991).

The tectostratigraphic units S2–S3 and S4 are interpreted as foredeep basins that migrated to the north because of at least four episodes of fold belt deformation and propagation of the mountain front toward the foreland (Mingramm, 1982; Biddle et al., 1986; Klepeis, 1994; Kraemer, 1998).

4. Structure

The regional transect analyzed here crosses the entire Patagonian Andes from the deformation front of the fold belt to the Pacific Ocean (Fig. 1).

The Patagonian Andes is divided into (1) an external domain or fold belt and (2) an internal or coastal domain. These two domains can be mapped regionally, and the boundary between them is the basement thrust front, which is usually a Cenozoic foreland vergent thrust that places basement rocks over Jurassic–Cretaceous sedimentary deposits (Ramos, 1979; Allen, 1982; Kraemer, 1998) (Fig. 1). Along the transect, the boundary is a foreland vergent basement thrust located at the north flank of the Cordillera Darwin (Klepeis, 1994), which is the highest elevation of the region and partially covered by perennial ice (Fig. 3).

4.1. External domain or fold belt

South of latitude 50°S, the Patagonian fold belt has a dominantly thin-skinned structural style coincident with a rapid increase in the total sedimentary thickness of the Magallanes basin to the south (Fig. 1). A seismic reflection profile along the Magallanes strait (Fig. 4(A)) shows a south-dipping basement that is not involved in the deformation and a sedimentary wedge that thickens from 4 km at the foreland to more than 10 km in the hinterland (Yañez et al., 1988). The deformation front of the fold belt consists of an open syncline, the erosion of which defines a surface correlative with the Neogene unconformity at the top of S4.

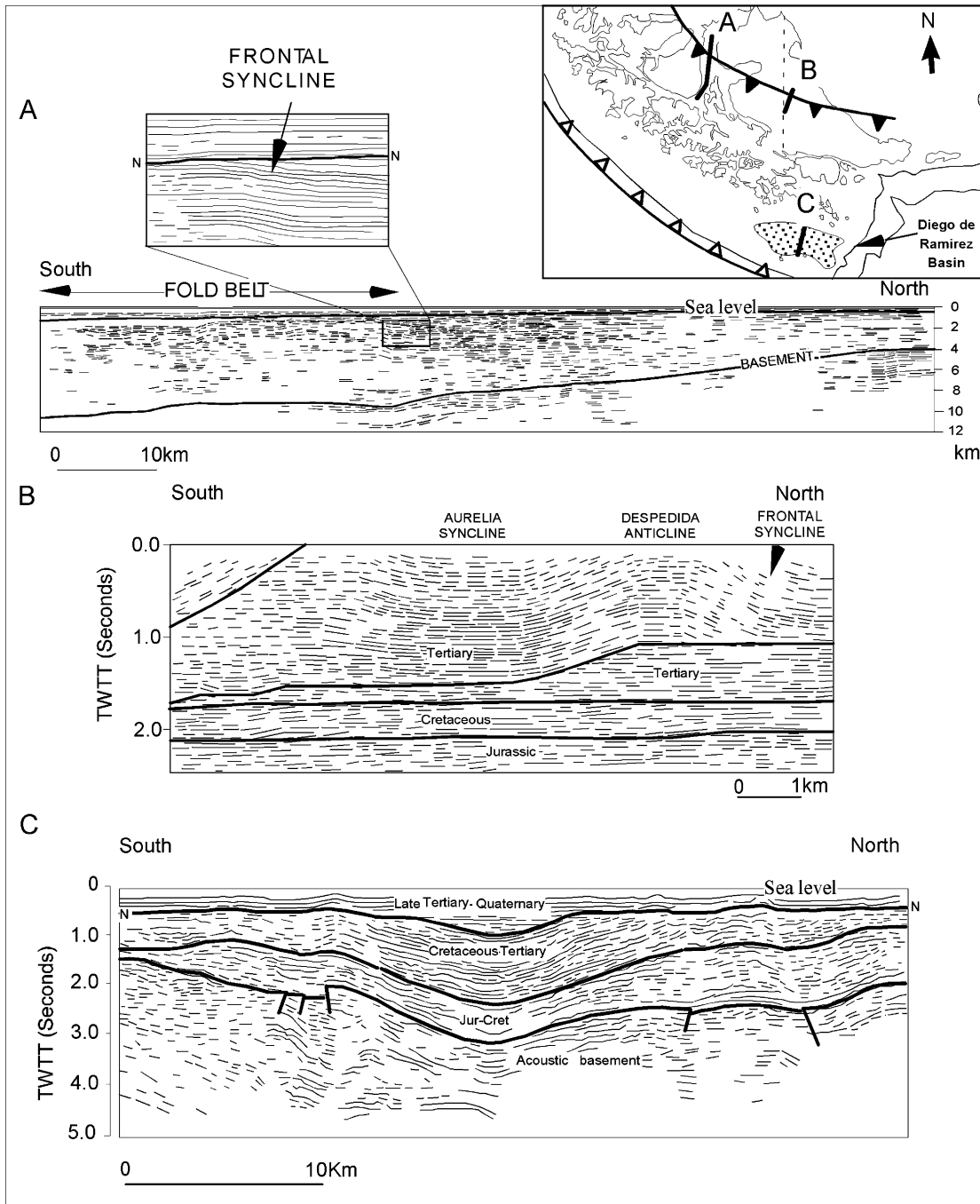


Fig. 4. (A) Tracing of a reflection seismic line along the Magallanes strait (from [Yañez et al., 1988](#)). The inset shows the frontal syncline and Neogene unconformity. Note the hinterland dipping basement below the deformed fold and thrust belt. (B) Tracing of a reflection seismic line along the frontal fold belt ([Cagnolatti et al., 1987](#)). Note the ramp-flat-ramp geometry and related fault bend fold in Tertiary sediments. (C) Tracing of a reflection seismic line across the Diego de Ramirez forearc basin ([González, 1989](#)). Note the slight compressive deformation compared with the frontal fold belt. N: Neogene unconformity.

Along the transect, a similar frontal syncline is observed at the north limb of the Despedida anticline ([Cagnolatti et al., 1987](#)) (Fig. 4(B)). To the south, three more anticlines involve Tertiary rocks ([Alvarez Marrón et al., 1993](#)) (region A in Fig. 5(A)).

The intensity of deformation increases to the south, exposing Upper Cretaceous rocks in an imbricated system

of north vergent thrust (region B in Fig. 5(A)), whereas a back thrust system exposes Lower Cretaceous rocks farther to the south (region C in Fig. 5(A)).

The Cerro Verde anticline, affected by Quaternary strike-slip faults at its northern flank, is the northernmost outcrop of the Tobifera Formation along the transect. The basement thrust located at the southern limb of the Cerro

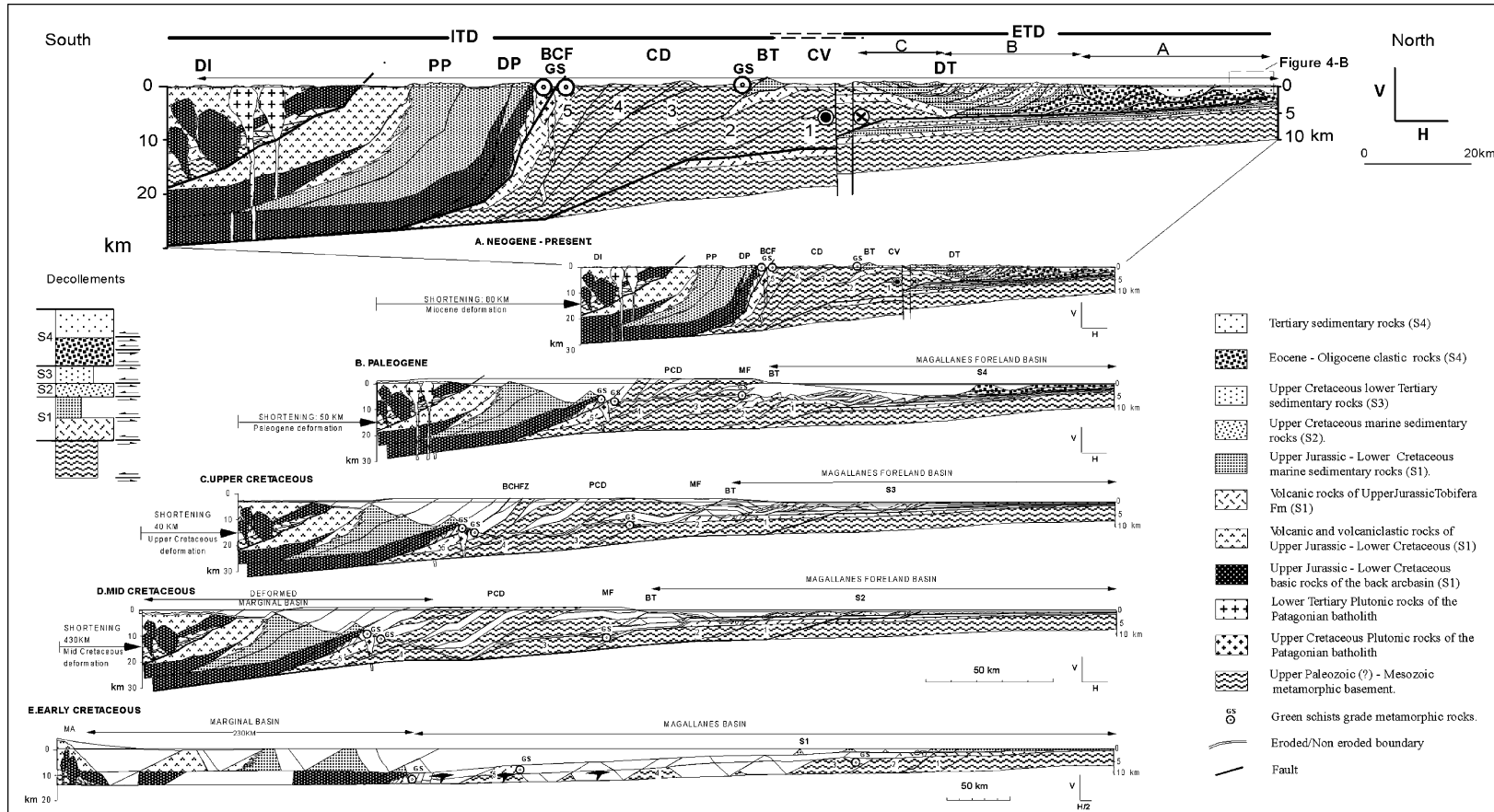


Fig. 5. (A) Regional cross-section showing the main Andean tectonic domains after the Neogene compressive deformation. ITD: Internal tectonic domain, ETD: external tectonic domain (fold and thrust belt). (A–C) Subregions of the fold belt. S1–S4: Tectonostratigraphic units. TDF: Tierra del Fuego, CV: Cerro Verde anticline, CD: Cordillera Darwin, BCFZ: Beagle Channel fault zone, PD: peninsula Dumas, PP: peninsula Pasteur, DI: Duperre Island, BT: basement thrust, MF: inferred position of mountain front, PCD: Protocordillera Darwin, MB: marginal basin, MGB: Magallanes basin, MGFB: Magallanes foreland basin, MA: magmatic arc (see Fig. 1 for geographic location). (B) Retrodeformed cross-section after the Paleogene compressive event. (C) Retrodeformed cross-section after the Upper Cretaceous–Paleogene compressive event. (D) Retrodeformed cross-section after the mid-Cretaceous compressive event. (E) Lower Cretaceous paleogeography.

Verde anticline (Klepeis, 1994) (BT in Fig. 5(A)) is the southern boundary of the external domain or fold belt (Figs. 3 and 5(A)).

4.2. Internal domain

Three main northwest–southeast-trending thrusts were mapped at the northeastern slope of the Cordillera Darwin (Caminos et al., 1981; Mingramm, 1982) (Fig. 3), of which the northernmost foreland vergent basement thrust (BT in Fig. 5) (Klepeis, 1994) forms the northern limit of the internal domain. The Beagle Channel fault zone, at the southern edge of the Cordillera Darwin, is a tectonic boundary associated with an abrupt change from chlorite–biotite grade on the north coast of isla Gordon to kyanite grade on the north shore of the Beagle Channel (Bruhn, 1979; Nelson et al., 1980; Nelson, 1982; Kohn et al., 1995). This discontinuity is not recognized in the transect (20 km to the east) because the rocks at the north coast of peninsula Dumas and the north shore of the Beagle Channel are both chlorite–biotite grade (Fig. 3).

South of the Beagle Channel, Mesozoic basic rocks of the Tortuga complex crop out along the north coast of peninsula Dumas, the southern coast of isla Navarino (Cunningham, 1993), and a large northwest–southeast-trending belt from isla Gordon to peninsula Tekenika (Suarez et al., 1985; Cunningham, 1994). The deformation and metamorphism of the basic rocks on isla Gordon precedes a granodioritic intrusion dated at 90.3 ± 0.4 Ma (Suarez et al., 1985).

4.3. Structural interpretation

The subsurface structural interpretation was performed by applying the kink method (Suppe, 1983). The geometric and kinematic compatibility of the interpretation was tested through the retrodeformation of the balanced cross-section in four stages.

4.3.1. Fold belt

The anticlines and synclines of the frontal fold belt (Fig. 3) were interpreted as fault bend folds and wedge structures (triangle zones) (Cagnolatti et al., 1987; Alvarez Marrón et al., 1993) related to three decollement levels at the top (D8), middle (D7), and base (D6) of the Eocene–Oligocene clastic deposits (region A in Fig. 5(A)).

The first two thrust sheets of the north vergent imbricated system (region B in Fig. 5(A)) transported Upper Jurassic–Lower Cretaceous rocks and merged into a decollement located at the top of the Tobifera Formation (D3), which was finally rooted in the basal decollement of the fold belt located at a deeper level in the basement (D1). The decollement at the top of the Tobifera Formation is exposed at the surface at the crest of the Cerro Verde anticline (dashed line in Fig. 5(A)) (Klepeis, 1994). The third thrust sheet of the north vergent imbricated system transported

deeper basement rocks and vulcanites of the Tobifera Formation that formed the core of the Cerro Verde anticline.

These three thrust sheets are interpreted as fault propagation folds. The northern sheet formed a wedge, detached in decollement D7 with a back thrust in the north limb, and affected finally by a late anticlinal breakthrough (Suppe and Medwedeff, 1990). The imbricated system of north vergent thrusts is bound to the south by the Desado thrust (DT in Fig. 5(A)), which is located at the northern limb of the Cerro Verde anticline. These thrust sheets transported Upper Jurassic–Lower Cretaceous rocks, merging the thrusts into a decollement located at the base of Lower Cretaceous shales (D3).

Along the northern coast of lago Fagnano and Seno Almirantazgo crops out a belt of Lower Cretaceous marine sediments, which is thrust over Upper Cretaceous deposits along the Desado thrust (Fig. 2) (Klepeis, 1994). The hanging wall of the Desado thrust is deformed by an imbricated system of back thrusts related to a decollement at the base of the Lower Cretaceous sediments (D3) (region C in Fig. 5(A)).

The Cerro Verde anticline, located along the southern coast of lago Fagnano (Klepeis, 1994), continues to the west along the Sierra Valdivieso (Caminos et al., 1981) (Fig. 2). The anticline is interpreted as two stacked, north vergent basement thrust sheets (thrust sheets 1 and 2 in Fig. 5(A)) that re-fold the previously deformed sedimentary cover and the decollement (D3) located at the top of the Tobifera Formation. The basement thrust sheets are interpreted as transported northward 45 km over the Cretaceous platform, which created 13 km of structural relief. They account for most of the shortening of the fold belt north of the Desado thrust.

4.3.2. Internal domain

The basement thrust that bounds the Cordillera Darwin on the north (BT in Fig. 5(A)) is interpreted as an out-of-sequence thrust uplifted during the Paleocene–Eocene (Klepeis, 1994). The Cordillera Darwin is the most important outcrop of low to high grade Cretaceous metamorphic basement in Tierra del Fuego (Nelson et al., 1980; Kohn et al., 1995). The outcrops of Jurassic volcanics at the northwest and southeast edges of Cordillera Darwin suggest a complex antiformal structure (Fig. 3).

Three northwest–southeast thrusts were mapped along the transect (Caminos et al., 1981; Mingramm, 1982) that are interpreted here as three north vergent, imbricated basement thrust sheets (thrust sheets 3, 4, and 5 in Fig. 5(A)) rooted in a basal decollement (D1) located 30 km below sea level. This decollement coincides with the strong reflector imaged beneath the Beagle Channel and the continental shelf of the continent at 8–13 sec for two-way travel time (> 20 km) (Cunningham, 1993). The three thrusts join west of Cordillera Darwin, and the shortening is probably transferred to other structures, such as the back thrusts recognized in Cordillera Darwin (Nelson et al., 1980) (BKT

in Fig. 3). A similar structural style was described in a section along the Gajardo Channel, 300 km to the northwest of the transect (Harambour, 2002). Thus, foreland vergent basement thrusts and back thrusts probably are common features in the internal domain.

Because of the intrusion of large Upper Cretaceous plutons and the pervasive strike–slip faulting that obliterated previous structures, mid-Cretaceous thrust faults that might have accommodated horizontal shortening during the closure of the marginal basin have not been demonstrated (Cunningham, 1994). However, the intense mid-Late Cretaceous compressive deformation in Cordillera Darwin (Nelson et al., 1980; Kohn et al., 1995), the deformation and metamorphism of basic rocks in isla Gordon (Cunningham, 1994), and the nearly 90° rotation of the magmatic arc (Cunningham et al., 1991) strongly suggest an intense tangential deformation accommodated by thrusting during the marginal basin closure.

The outcrops of the Upper Jurassic Tobifera Formation, covered by basic rocks of the Tortuga complex along the coast of peninsula Dumas (Suarez et al., 1985), are interpreted as the leading edge of a thrust sheet composed of transitional and oceanic crust detached at the base of the basic rocks and thrust over the continental crust of Cordillera Darwin along the Beagle Channel fault (Fig. 5(A)).

Both the hanging and footwall rocks of the Beagle Channel fault are chlorite–biotite grade along the transect, which suggests a limited amount of postmetamorphic reverse displacement. However, 20 km west of the transect, where the Cordillera Darwin reaches its maximum north–south width, topographic height, and structural relief the hanging wall of the Beagle Channel fault remains chlorite–biotite grade, whereas the footwall exposes high grade rocks with kyanite. This trend may be due to a Cretaceous postmetamorphic episode of extensional displacement along the Beagle Channel fault (Nelson, 1982; Dalziel and Brown, 1989).

South of the Beagle Channel, basic rocks of the Tortuga complex outcrop in northwest–southeast-trending belts along the southern coast of isla Navarino and isla Gordon. Basic rocks strongly foliated and mylonitized prior to 90.3 ± 0.4 Ma record the mid-Cretaceous closure of the marginal basin (Cunningham, 1993).

The disharmonic style between the intensely folded Lower Cretaceous turbidites and the less folded basic rocks below suggest a decollement located at the contact between the units (Bruhn, 1979). A decollement is inferred from the contact between the coarse supra fan and middle fan facies of the Lower Cretaceous turbidites along the peninsula Pasteur (Suarez et al., 1985). Such an inference is based on the enormous thickness (>12 km) that would result if they were considered a continuous stratigraphic succession (Fig. 5(A)).

As a working hypothesis, it is postulated that the oceanic rocks of the Tortuga complex, the Lower Cretaceous

vulcaniclastic rocks, and the turbidites are part of an allochthonous unit that was ‘passively’ transported to the continent by the continued deformation of the fold belt during the Late Cretaceous–Tertiary (Fig. 5(A)). This hypothesis is supported by a gravimetric survey south of Tierra del Fuego that indicates the absence of high density rocks underneath the deformed marginal basin (Suarez et al., 1985).

The thick deposits affected by gentle flexures, as imaged in seismic sections at the Diego de Ramirez basin (Fig. 4(C)), indicate that the forearc region was a relatively subsiding and stable region. In contrast, the Andean internal orogenic domain underwent intense deformation and exhumation during Mesozoic and Cenozoic times (Fig. 5(A)).

5. Estimation of orogenic shortening

The balanced cross-section of Fig. 5(A) records several different episodes of geologic evolution in the Patagonian Andes. To calculate the orogenic shortening produced by each compressive event, four retrodeformed cross-sections were elaborated by sequentially restoring the tectostratigraphic units from the youngest to the oldest (S4 to S1) (Fig. 5(B)–(E)). The paleomountain front of each stage was located in the region between the last noneroded remnant of the syn to postorogenic deposits and the closest documented active thrust or source area.

The construction of retrodeformed cross-sections and the balance of the structures above the erosion level was used to test the kinematic compatibility between successive stages. In the internal domain, a maximum burial of 26–30 km calculated from thermobarometry and P – T path (Kohn et al., 1995) provided an estimation of the vertical overburden during some stages.

The cross-section of Fig. 5(A) was divided into internal and external domains, which are mappable units defined by the distribution of lithologic associations and structural style. The cross-sections of Fig. 5(B)–(D) show the restoration of the Neogene, Eocene, and Maastrichtian–Paleocene compressive events, as well as the progressive backward displacement of each mountain front from the foreland to the hinterland. The cross-section of Fig. 5(E) shows the restoration of the mid-Cretaceous event of deformation and the Early Cretaceous paleotectonic units of the extensional stage. These units include a back arc basin developed over continental crust, or Magallanes basin; a back arc basin floored by oceanic crust, or ‘Rocas Verdes marginal basin;’ and a magmatic arc (Dalziel et al., 1974; Suarez and Pettigrew, 1976; Suarez, 1979; Dalziel, 1981).

The subsurface interpretation and shortening estimation is progressively less constrained toward the south. The main uncertainties are the estimation of the maximum width reached by the oceanic back arc basin, the deep geometry of

thrusting in Cordillera Darwin, and rock movement out of the plane of the section due to strike–slip faulting. This uncertainty is reflected in the broad range of the total amount of shortening calculated along the transect, which ranges from a maximum of 600 km to a minimum of 300 km.

5.1. Neogene stage

The Neogene event of deformation produced an estimated shortening of 80 km (Fig. 5(A)). Sixty kilometers of the shortening were produced by the foreland-directed thrusting of the basement thrust sheets of Cerro Verde anticline, and 20 km were related to a partial reactivation of preexisting faults (Fig. 5(B)). During the Neogene stage, 13 km of structural relief were created between the basement of the Cordillera Darwin and the basement of the fold and thrust belt.

5.2. Paleogene stage

The Paleogene event of deformation produced a shortening of 50 km (Fig. 5(B)). This section shows the location of the mountain front and the foreland basin at the end of the deposition of the Eocene–Oligocene clastic rocks (S4). The displacement along the five main basement thrusts (1–5 in Fig. 5(C)) accounts for most of the Paleogene shortening. The displacement for thrusts 1 and 2 produced the proto-Cerro Verde anticline, in that the shortening was partially transferred to the thin-skinned, transported fault propagation folds located farther north (Fig. 5(B)).

Displacement along basement thrusts 3–5 produced the Paleocordillera Darwin, the southern sedimentary source for the Eocene clastic deposits of S4 (Hoffstetter et al., 1957). The pulse of rapid exhumation and cooling between 60 and 40 Ma (Upper Paleocene to Lower–Middle Eocene) in Cordillera Darwin (Nelson, 1982; Kohn et al., 1995) can be related to the foreland out-of-sequence thrusting and uplift of Cordillera Darwin (Klepeis, 1994), mainly along basement thrust 3 (BT) (Fig. 5(B) and(C)).

5.3. Late Cretaceous stage

The Late Cretaceous event of deformation produced a shortening of 40 km (Fig. 5(C)). This section shows the location of the mountain front and the foreland basin at the end of deposition of S3, which has much less thickness than S4. The displacement for basement thrusts 3 and 4 accounts for most of the shortening in this stage.

5.4. Mid-Cretaceous stage

The restoration shows that the mid-Cretaceous event of deformation produced a maximum shortening of 430 km (Fig. 5(D)). This section shows the location of the mountain front and the foreland basin at the end of the deposition of

the Upper Cretaceous tectostratigraphic unit S2. It is by far the most significant in terms of the paleogeographic changes and intensity of deformation. A period of basement thrusting and metamorphism, followed by a period of rapid exhumation and cooling in Cordillera Darwin (Nelson et al., 1980; Kohn et al., 1995), coincides with an episode of fast subsidence and deposition of deep ocean turbidites in the Magallanes foreland basin (Natland et al., 1974; Biddle et al., 1986).

The basic rocks of the Tortuga complex probably represent the upper 5 km of the oceanic basin crust (layers 1, 2 and 3) detached from the oceanic lithosphere.

The maximum shortening of 430 km is partitioned into 230 km related to the closing of the marginal basin and 200 km related to the basement thrusting in Cordillera Darwin. The shortening estimation at the mid-Cretaceous stage was calculated using techniques of cross-section balancing applied to the available surface information. Assuming that the present width of outcropping basic rocks and the historical width of the oceanic back arc basin are approximately the same (25 km) and admitting a shortening overestimation of 50% in Cordillera Darwin, a minimum value of 100 km of shortening seems reasonable for this stage.

5.5. Early Cretaceous stage

This stage shows the full restoration of S1 deposited in the marginal basin, floored by oceanic crust, and the Magallanes basin over the attenuated continental crust during the climax of the rifting stage (Fig. 5(E)). The marginal basin is filled with Upper Jurassic–Lower Cretaceous volcanic, volcanoclastic, and deep ocean turbidites from the magmatic arc, and the Magallanes basin is filled with ocean turbidites and shallow marine sediments from the foreland.

6. Implications of the shortening calculated. Balance at crustal scale and palinspastic restoration of the Patagonian orocline

6.1. Area balance at crustal scale

The problem of mass balance with a shortened fold belt above a less shortened basement in the Patagonian Andes was first addressed by Winslow (1981). To analyze the crustal area balance, we constructed an evolutive sketch of sections at lithospheric scale from the present to the Early Jurassic (Fig. 6). We assumed that the continental crustal area (Ac) under the basal decollement remains constant throughout the evolutive sketch and that magmatic addition is neglected (Fig. 6).

Section A shows the forearc, the magmatic arc, and the deformed back arc bound by oceanic subduction directed to the north. Assuming Airy isostatic compensation of

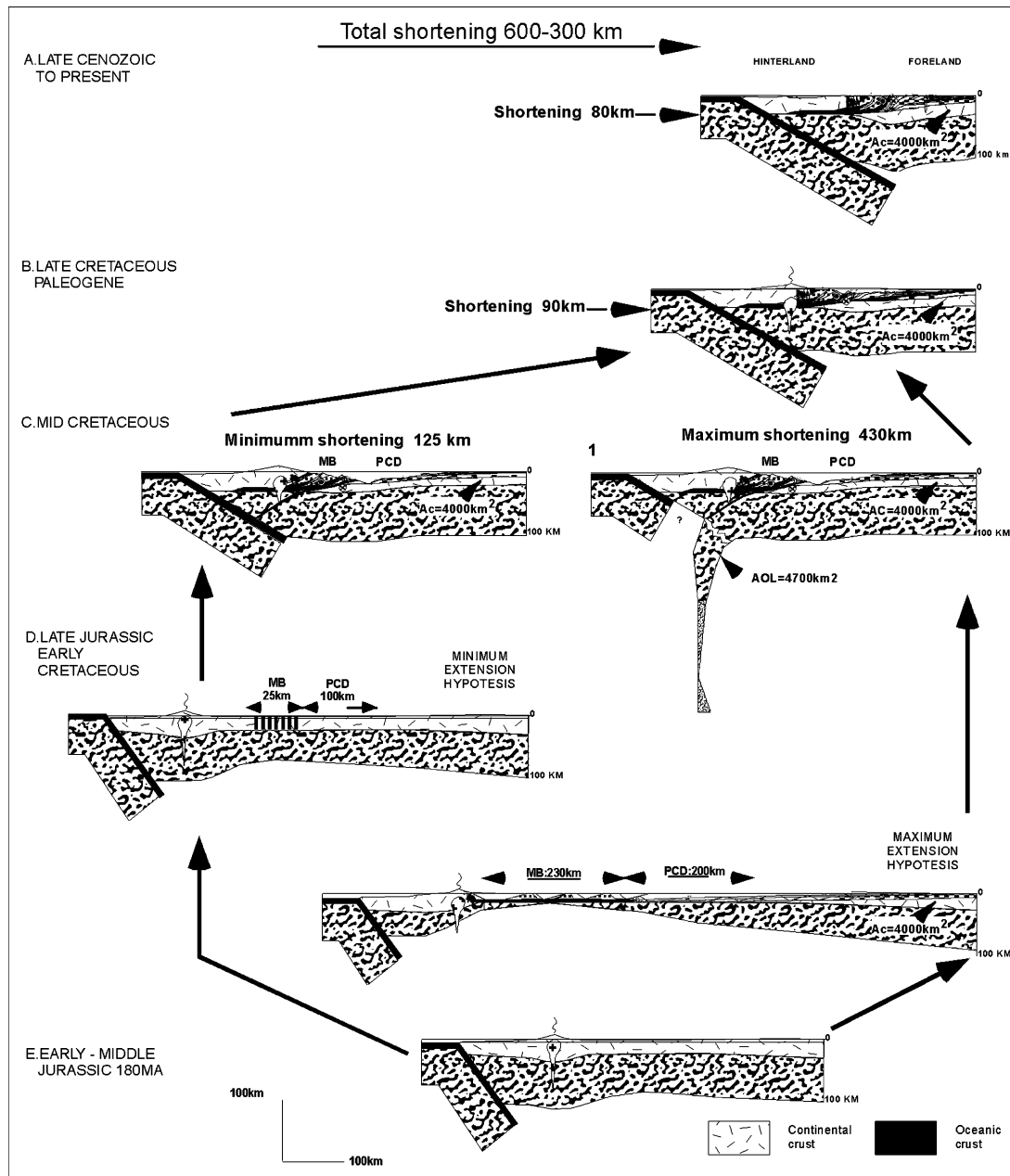


Fig. 6. Sections showing the mass balance at crustal scale. (A) Late Cenozoic to present stage. The oceanic crust of the marginal basin is emplaced over continental crust. The constant area of continental crust (A_c) below the basal decollement is 4000 km^2 . The accumulated shortening is between 600 and 300 km, and the Cenozoic deformation is 80 km. (B) Late Cretaceous–Paleogene stage. The shortening is 90 km. (C) Mid-Cretaceous arc-continent collision stage. The maximum shortening estimated at this stage is 430 km (C1), which corresponds to 230 km from the closure of the marginal basin and 200 km from the shortening of the Protocordillera Darwin (PCD). The minimum shortening estimated at this stage is 100 km (C2), which corresponds to 0 km from the marginal basin and 100 km from the PCD. (D) Late Jurassic–Early Cretaceous back arc rifting stage. In the maximum extension hypothesis (D1), the back arc is retrodeformed 430 km, 230 km to the marginal basin and 200 km to the restored continental and transitional crust of the Magallanes basin. In the minimum extension hypothesis (D2), the back arc basin reaches a width of 25 km, and the PCD 100 km. (E) Early Jurassic stage. The extension of the continental crust and oceanic crust of the marginal basin is removed. This stage corresponds to the beginning of the crustal extension and associated volcanism of the Tobifera Formation. MB: Marginal basin.

the maximum topography of Cordillera Darwin ($h_i = 2400 \text{ m a.s.l.}$), the maximum local crustal root is nearly 15 km, and the crustal area at this stage is 4000 km^2 . Section B shows the removal of 80 km of Late Cenozoic shortening in the fold belt with continued oceanic subduction under the continent. In section C, 90 km of Late

Cretaceous–Paleogene shortening is removed from the fold belt. This stage shows the configuration after the mid-Cretaceous arc-continent collision. The maximum shortening estimated at this stage is 430 km (Fig. 6(C1)), which corresponds to 230 km of the closure of the marginal basin (MB) and 200 km of the Protocordillera Darwin (PCD) to

the north. Because of the amount of crustal shortening and assuming that the thickness of the lithospheric mantle is constant through time, 4700 km² of lithosphere (AOL) should be remobilized for balance. One possible mechanism is to subduct and detach the excess of lithosphere, a process that has been proposed to explain the isostatic rebound and uplift in Cordillera Darwin (Cunningham, 1995). The mass balance of the subdecollent continental crust between stages D and C can be attained by underthrusting continental crust under the marginal basin.

The minimum shortening estimated at this stage is 100 km (Fig. 6(C2)), which corresponds to 0 km of the back arc basin and 100 km of the PCD. Because of the small amount of shortening assumed, all crustal shortening is balanced by lithospheric thickening, and no other mechanisms are necessary to maintain the area balance.

Section D shows the Late Jurassic–Early Cretaceous paleogeography obtained by the removal of 230 km of shortening in the marginal basin and 200 km of shortening in the PCD. The marginal basin reached a maximum width of 230 km, and the Magallanes basin achieved its maximum stretching at the oceanic-continental back arc transition. Section E shows the Early Jurassic paleotectonic domains and

the continental back arc before the crustal stretching related to the rifting stage of the Magallanes basin (Fig. 6(E)).

The maximum shortening hypothesis precludes the obduction of the oceanic lithosphere over the continent as a mechanism to close the marginal basin and suggests that the basic rock vestiges of the marginal basin are placed entirely over continental crust. This explains the absence of important positive gravimetric anomalies south of Cordillera Darwin (Suarez et al., 1985). However, it remains unclear why the oceanic lithosphere was delaminated at the contact between the basic and ultrabasic rocks. This hypothesis explains the isostatic rebound and erosion of Cordillera Darwin as a consequence of thickening by thrusting but requires a short-lived oceanic reverse subduction episode to balance the areas during orogenic contraction.

The minimum shortening hypothesis explains the absence of ultrabasic rocks in the surface and does not require reverse subduction or other processes for balance. However, the absence of positive gravimetric anomalies associated with the marginal basin, the mechanisms that explain the crustal thickening in Cordillera Darwin, and post-folding tectonic rotations of 90° remain unclear.

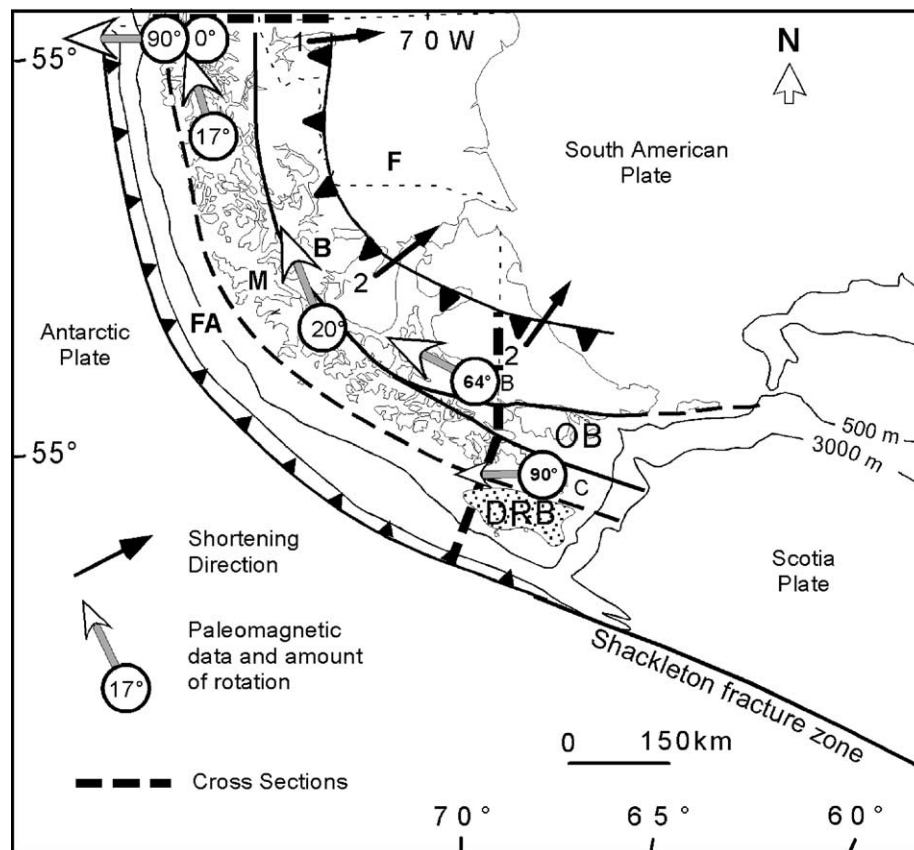


Fig. 7. Map of the Patagonian orocline showing the tectostratigraphic regions mapped. FA: forearc, M: magmatic arc, B: back arc, OB: back arc oceanic crust remnants, DRB: Diego de Ramirez forearc basin, and F: stable foreland. Black arrows indicate the shortening direction obtained from the kinematic analysis of minor faults from Diraison et al. (2000) and Kraemer (1991). Open arrows indicate paleomagnetic directions and amount of rotation (Dalziel et al., 1973; Burns et al., 1980; Cunningham et al., 1991; Rapalini et al., 2001). Dashed lines are the balanced regional cross-sections used to estimate the orogenic shortening.

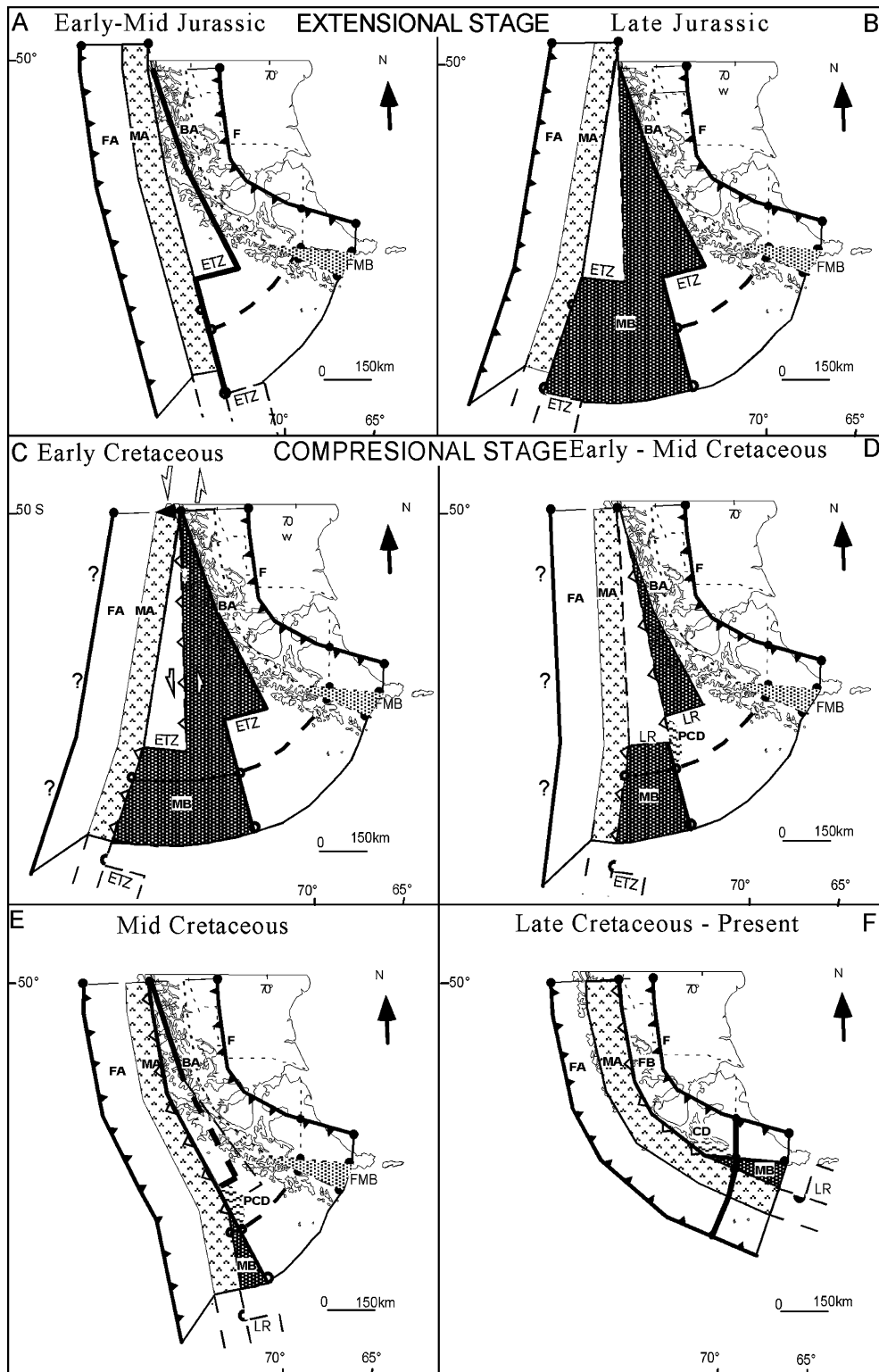


Fig. 8. Palinspastic reconstruction of the Patagonian orocline. ETZ: extensional transfer zones, LR: lateral ramps, FA: forearc, MA: magmatic arc, BA: back arc, MB: marginal basin, F: present foreland fold belt front, FMB: future location of the deformed marginal basin. The dashed line is the restored regional cross-section. Extensional stage: (A) Early Jurassic back arc extension with 'tooth and socket' geometry in the initial rifting pattern. Straight rift segments are connected by transverse ETZs. (B) Late Jurassic–Early Cretaceous opening of the oceanic back arc basin and clockwise rotation of the magmatic arc. The basin reached a width of 230 km. Compressional stage: (C) Transpressive closing of the oceanic back arc basin and the beginning of a counterclockwise rotation of the magmatic arc. Note the mismatch between the opposite margins of the basin. (D) Initial local arc-continent collision, rotation of the arc, and formation of the Protocordillera Darwin (PCD), bounded by LRs. (E) Complete closing of the marginal basin and deformation of Cordillera Darwin during the mid-Cretaceous with a shortening of 430 km along the section. (F) Deformation of the fold belt with a shortening of 170 km and final rotation of the arc.

6.2. Palinspastic restoration of the Patagonian orocline

Paleomagnetic studies (Dalziel et al., 1973; Burns et al., 1980; Cunningham et al., 1991; Rapalini et al., 2001) and paleogeographic reconstructions (Dalziel et al., 1974; Dalziel, 1981; Diraison et al., 2000) suggest that the present bending of nearly 90° at 56°S is a consequence of a counterclockwise tectonic rotation of a mountain belt that was nearly rectilinear or slightly curved in Mesozoic time. The southward increase in the tectonic rotation is coeval with an increase in the amount of total orogenic shortening estimated, from 110 km at 50°SL (Kraemer et al., 1996) to 600 (maximum)–300 km (minimum) at 56°SL.

These data and all available geologic information were combined to generate six palinspastic maps of the Patagonian orocline that show the paleoposition of the magmatic arc, the back arc basin, and the fold belt from the Jurassic to the present.

The first step in the construction of the palinspastic maps was the regional mapping of the three main tectonostratigraphic domains of the Patagonian orocline: the forearc, the magmatic arc, and the back arc region. Paleomagnetic data and shortening directions then were plotted in their corresponding geographic locations (Fig. 7).

The palinspastic reconstruction of the orocline (Fig. 8) eliminated the deformation of the fold belt, opened the oceanic back arc basin, and straightened the magmatic arc to the position that corresponds with the climax of the extensional stage.

There are three quantitative constraints of the restoration. First, the amount of shortening increases from 110 km at 50°SL (Kraemer et al., 1996) to 600–300 km at 56°SL. Second, the direction of shortening of the fold belt, obtained from the kinematic analysis of minor faults, is subperpendicular to the mountain belt (Kraemer, 1991; Diraison et al., 2000). Third, the rotational component obtained from paleomagnetic studies is 17° in isla Rennell (51°30'S) (Dalziel et al., 1973), 64° at the north edge of Cordillera Darwin (54°30'S) (Burns et al., 1980), and 90° in isla Hoste (55°30'S) (Cunningham et al., 1991).

The main assumptions of the palinspastic reconstruction are as follows:

1. The plan view area of the forearc and magmatic arc remained constant during the different stages. For simplicity, it was assumed that the dominant process of deformation was simple shear parallel to the mountain belt but strike–slip deformation perpendicular to the axis of the magmatic arc or strike–slip oroclinal bending (Cunningham, 1995), it is also a mechanism of deformation compatible with the palinspastic reconstruction presented here. Both mechanisms provide an explanation for large, local, counterclockwise rotations measured at 50° in the forearc region (Rapalini et al., 2001). The shortening perpendicular to the magmatic arc and forearc was negligible, as supported by the scarce

compressive deformation observed in seismic lines across the Diego de Ramirez forearc basin (González, 1989), the preservation of forearc sedimentary rocks accreted during Jurassic time (Forsythe and Mpodozis, 1979), and the open folding described in arc-related volcanic rocks in peninsula Hardy (Suarez et al., 1985).

2. The plan view area of the back arc region changed because of intense compressive deformation. During the extensional stage, new crust was created from the opening of the oceanic back arc basin (Katz, 1972; Dalziel et al., 1974; Bruhn et al., 1978; Dalziel, 1981) and was consumed during the mid-Cretaceous closing of the basin. The initial rifting pattern in the back arc region may have had a ‘tooth-and-socket’ geometry. This premise provides an explanation for the localized occurrence of the metamorphic core of Cordillera Darwin. The central rift of the back arc basin may have been offset by extensional transfer zones that produced a basin with tooth-like margins. If the compressional deformation during the back arc basin closing had a component of left-lateral displacement, as is the case in the Patagonian Andes (Cunningham, 1993; 1995), the teeth of one margin would not fit into the socket of the opposite margin, which would lead to localized crustal thickening, metamorphism, exhumation, and, eventually, extensional collapse (Coward et al., 1991; Coward, 1996). These phenomena have been described and proposed for the Cordillera Darwin (Nelson et al., 1980; Nelson, 1982; Dalziel and Brown, 1989; Kohn et al., 1995).
3. After the mid-Cretaceous tectonic event, the deformation was concentrated in the back arc region, and the fold belt was built by several pulses of compressive deformation above a basal decollement (Mingramm, 1982; Winslow, 1982; Kraemer, 1991; Alvarez Marrón et al., 1993; Klepeis, 1994). The deformation was partitioned into broadly distributed shortening in the back arc basin and fold belt, whereas the strike–slip displacement was concentrated in a narrow zone at the continental side of the oceanic back arc or Beagle Channel fault zone. The thrust fault ‘fanning’ around a pole of rotation obtained in experimental models (Diraison et al., 2000) is a first-order mechanism that explains the southward increase in fold belt shortening.

Although the construction of the palinspastic maps was detailed from the present to the past, the description presented here will progress from the Jurassic extensional stage to the present (Fig. 8(A)–(F)).

6.3. Palinspastic reconstruction

6.3.1. Extensional stage

Prior to the opening of the marginal basin, the Jurassic paleogeography consisted of a forearc, a magmatic arc, and a stretched continental crust in the back arc. The heavy

black line in Fig. 8(A) is the postulated rift pattern of the marginal basin with two straight segments linked by an extensional transfer zone.

During the Late Jurassic–Early Cretaceous, the magmatic arc rotated clockwise, opening the 230 km wide oceanic back arc basin, if we assume a maximum shortening hypothesis. Petrochemical data suggest that the back arc basin widened and its mafic igneous floor became more oceanic southward. Older ages obtained southward also suggest that the basin may have opened by unzipping from south to north (Stern et al., 1991). A similar conclusion was proposed on the basis of sedimentological criteria (Winn, 1978), and paleogeographic sketches show general similar geometries (Dalziel et al., 1974; Dalziel, 1981; Diraison et al., 2000). Previous estimations of the width of the oceanic back arc basin vary between 250–300 km (Winn, 1978) and 100–150 km (Dalziel et al., 1974). The maximum width of 230 km obtained from the restoration of the marginal basin explains paleomagnetic rotations of 90°, assuming that a straightened magmatic arc at the time of formation of the back arc basin was bent after magnetization and during basin closure (Cunningham, 1995). If we assume a minimum shortening hypothesis, the marginal basin reached a maximum width of 25 km; this stage would be represented by Fig. 8(E). If this is the case, the predicted paleomagnetic rotation is 30° less than the 90° measured, and some local block rotation, not observed in the field, is required to explain the difference.

As a consequence of the rifting geometry, the eastern continental margin of the oceanic back arc basin showed a reentrant to the north and a promontory to the south, whereas the western margin of the basin had a promontory (or a slice of the back arc attached to the magmatic arc to the north) and a reentrant to the south (Fig. 8(B)).

6.3.2. Compressional stage

During the Early Cretaceous, the oceanic back arc basin ceased its opening and started a compressional stage with a component of lateral displacement. At this stage, the sedimentary infill and oceanic crust of the basin was deformed, but the continental crust of the basin margins did not collide. The southern part of the magmatic arc reached a maximum rotation of nearly 90° with respect to its present position following a period of counterclockwise rotation (compare Fig. 8(C) and (F)).

Because of the left-lateral displacement between the basin margins, the promontory of stretched continental crust does not fit back into the reentrant of the opposite margin, thus leading to a localized collision and crustal thickening in the PCD (Fig. 8(D)).

When the promontories collided, the marginal basin along the section was shortened 230 km and the PCD 200 km. The northern part of the oceanic back arc basin was reduced to a narrow, discontinuous belt, whereas the less shortened southern zone remained a triangular zone of deformed oceanic rocks (Fig. 8(E)). After this stage, the magmatic arc

rotated progressively, the thickened crust of the PCD was exhumed, and the fold belt was shortened 170 km in three events of compressive deformation that propagated the deformation toward the foreland (Fig. 8(F)).

The extensional transfer zones inherited from the rifting stage may have acted as structural boundaries (lateral ramps) for the PCD, as well as a weakness zone that led to the opening of the Scotia Sea during the transpressive deformation of the Patagonian Andes during the Cenozoic.

7. Conclusion

The tectonic evolution of the Patagonian Andes of Tierra del Fuego includes an Upper Jurassic rifting episode followed by at least four Mesozoic–Cenozoic compressive events.

We estimate a maximum shortening of 600 km and a minimum shortening of 300 km, distributed as follows: 430 km during the mid-Cretaceous, 40 km during the Late Cretaceous, 50 km during the Paleogene, and 80 km during the Neogene. We used a regional balanced cross-section and its subsequent restoration in four stages.

A set of evolutive profiles at lithospheric scale from the Jurassic to the present show that, assuming a maximum shortening of 600 km, area balance is attained only if the back arc lithosphere created during the early rifting stage was partially consumed by a short episode of reverse subduction during the mid-Cretaceous compressive event.

The estimated orogenic shortening of 600 km was integrated into a more regional view by palinspastically restoring the Patagonian Andes orocline. The maximum shortening estimated herein is geologically reasonable and can explain the rotations of nearly 90° obtained from paleomagnetic studies in the magmatic arc.

Acknowledgements

This work was partially funded by the Consejo Nacional de Investigaciones Científicas y Técnicas de Argentina, P.I.A No. 151/92 to A. Mingramm. The author acknowledges Shell Argentina for permission to consult an unpublished report of A. Mingramm, who was a pioneer in applying the cross-section balancing techniques to the understanding of the geologic evolution of the Andes. I also acknowledge the helpful comments of K. Kleppeis and J. Suppe. Critical reviews by Jonas Kley and an anonymous reviewer are much appreciated.

References

- Aguirre Urreta, M.B., 1990. Paleogeography and biostratigraphy of the Austral basin in Argentina and Chile: an appeal for sound systematics. *Episodes* 13 (4), 247–255.

- Aguirre Urreta, M.B., Ramos, V.A., 1981. Estratigrafía y paleontología de la Alta Cuenca del Río Roble, Provincia de Santa Cruz. *Septimo Congreso Geológico Argentino* 3, 101–138.
- Allen, R.B., 1982. Geología de la Cordillera Sarmiento. *Boletín del Servicio Nacional de Geología y Minería* 38, 1–46.
- Alvarez Marrón, J., McClay, K.R., Harambour Palma, S.M., Rojas, L., Skarmeta, J., 1993. Geometry and evolution of the frontal part of the Magallanes foreland thrust and fold belt (Vicuña area), Tierra del Fuego, Southern Chile. *American Association of Petroleum Geologists Bulletin* 77 (11), 1904–1921.
- Arbe, H.A., 1989. Estratigrafía, discontinuidades y evolución sedimentaria del Cretácico en la Cuenca Austral, Provincia de Santa Cruz. In: Chebli, G., (Ed.), *Cuencas Sedimentarias Argentinas*, Universidad Nacional de Tucumán, pp. 419–442.
- Arbe, H.A., Hechem, J.J., 1984. Estratigrafía y facies de depósitos marinos profundos del Cretácico superior, Lago Argentino, Provincia de Santa Cruz. *9th Congreso Geológico Argentino Actas* 5, 7–14.
- Biddle, K.T., Uliana, M.A., Mitchum, R.M. Jr., Fitzgerald, M.G., 1986. The stratigraphic and structural evolution of the central and eastern Magallanes basin. In: Allen, A., Homewood, P. (Eds.), *Foreland Basins*, Blackwell Scientific Publications, Oxford, pp. 41–61.
- Bruhn, R.L., 1979. Rock structures formed during back-arc deformation in the Andes of Tierra del Fuego. *Geological Society of America Bulletin* 90 (2), 998–1012.
- Bruhn, R.L., Stern, C.R., de Wit, Y.M.J., 1978. Field and geochemical data bearing on the development of a Mesozoic volcano-tectonic rift zone and back arc basin in southernmost South America. *Earth and Planetary Science Letters* 41, 32–46.
- Burns, K.L., Rickard, M.J., Belbin, L., Chamalun, F., 1980. Further palaeomagnetic confirmation of the Magallanes orocline. *Tectonophysics* 63, 75–90.
- Cagnolatti, M., Covellone, G., Erlicher, J., Fantin, F., 1987. Fallamiento y plegamiento de cobertura al suroeste del río Grande, Cuenca Austral-Tierra del Fuego. *10th Congreso Geológico Argentino* 1, 149–152.
- Caminos, R., 1980. Andes Patagónico Fueguinos. In: Turner, J.C., (Ed.), *Segundo Simposio de Geología Regional Argentina*, vol. 2. Academia Nacional de Ciencias de Córdoba, pp. 1463–1501.
- Caminos, R., Haller, M.H., Lapido, O., Lizuain, A., Page, R., Ramos, V.A., 1981. Reconocimiento geológico de los Andes Fueguinos, Territorio Nacional de Tierra del Fuego. *7th Congreso Geológico Argentino* 3, 759–786.
- Coward, M.P., 1996. Balancing sections through inverted basins. In: Buchanan, P.G., Nieuwland, D.A. (Eds.), *Modern Developments in Structural Interpretation, Validation and Modelling*, Geological Society London, London.
- Coward, M.P., Gillcrust, R., Trudgill, B., 1991. Extensional structures and their tectonic inversion in the Western Alps. *J. Brooks Special Publication*, Geological Society London 56, 264.
- Cunningham, W.D., 1993. Strike-slip faults in the southernmost Andes and development of the Patagonian orocline. *Tectonics* 12 (1), 169–186.
- Cunningham, W.D., 1994. Uplifted ophiolitic rocks on Isla Gordon, southernmost Chile: implications for the closure history of the rocas Verdes marginal basin and the tectonic evolution of the Beagle Channel region. *Journal of South American Earth Sciences* 7 (2), 135–147.
- Cunningham, W.D., 1995. Orogenesis at the southern tip of the Americas: the structural evolution of the Cordillera Darwin metamorphic complex, southernmost Chile. *Tectonophysics* 244, 197–229.
- Cunningham, W.D., Klepeis, K.A., Gose, W.A., Dalziel, I.W.D., 1991. The Patagonian orocline: new paleomagnetic data from the Andean magmatic arc in Tierra del Fuego, Chile. *Journal of Geophysical Research* 96 (B10), 16061–16067.
- Dalziel, I.W.D., 1981. Back-arc extension in the southern Andes, a review and critical reappraisal. *Philosophical Transactions of Royal Society of London A* 300, 319–335.
- Dalziel, I.W.D., Brown, R.L., 1989. Tectonic denudation of the Cordillera Darwin metamorphic core complex, Tierra del Fuego: implications for cordilleran orogenesis. *Geology* 17, 699–703.
- Dalziel, I.W.D., Cortés, R., 1972. Tectonic style of the southernmost Andes and the Antarcticandes. *24th International Geological Congress Section* 3, 316–327.
- Dalziel, I.W.D., Palmer, K.F., 1979. Progressive deformation and orogenic uplift at the southernmost extremity of the Andes. *Geological Society of America Bulletin* 90, 259–280.
- Dalziel, I.W.D., Kligfield, R., Lowrie, W., Opdike, N.D., 1973. Palaeomagnetic data from the southernmost Andes and the Antarcticandes. In: Tarling, D.H., Runcorn, S.K. (Eds.), *Implications of Continental Drift to the Earth Sciences*, vol. 1. Academic Press, San Diego, CA, pp. 87–101.
- Dalziel, I.W.D., De Wit, M.F., Palmer, K.F., 1974. Fossil marginal basin in the southern Andes. *Nature* 250, 291–294.
- Diraison, M., Cobbold, P.R., Gapais, D., Rosello, E., 2000. Cenozoic crustal thickening, wrenching and rifting in the foothills of the southernmost Andes. *Tectonophysics* 316, 91–119.
- Forsythe, R., Mpodozis, C., 1979. El archipiélago Madre de Dios, Patagonia Occidental, Magallanes. Rasgos generales de la estratigrafía y estructura del basamento pre Jurásico superior. *Revista Geológica de Chile* 7, 13–29.
- González, E., 1989. Hydrocarbon resources in the coastal zone of Chile. In: Ericksen, G.E., Cañas Pinochet, M.T., Reinemund, J.A. (Eds.), *Geology of the Andes and its Relation to Hydrocarbon and Mineral Resources*, vol. 11. Circum-Pacific Council for Energy and Mineral Resources, pp. 383–404.
- Halpern, M., 1973. Regional geochronology of Chile south of 50° latitude. *Geological Society of America Bulletin* 84, 2407–2422.
- Halpern, M., Rex, D.C., 1972. Time of folding of the Yahgan formation and age of the Teckenika bed, southern Chile, South America. *Geological Society of America Bulletin* 83, 1881–1886.
- Harambour, S.M., 2002. Mega backfolding in the inner part of Magallanes fold and thrust belt, Gajardo channel, Magallanes Chile. *15 Congreso Geológico Argentino*, Comunicación, 383.
- Hervé, F., Nelson, E.P., Kawashita, K., Suarez, M., 1981a. New isotopic ages and the timing of orogenic events in the Cordillera Darwin, southernmost Chilean Andes. *Earth and Planetary Science Letters* 55, 257–265.
- Hervé, F., Davidson, J., Mpodozis, E., Covacevich, E.V., 1981b. The late Palaeozoic in Chile: stratigraphy, structure and possible tectonic framework. *Anais Academia Brasileira de Ciências* 53 (2), 361–373.
- Hoffstetter, R., Fuenzalida, H., Cecioni, G., 1957. *Lexique Stratigraphique International*. Amérique Latine, Centre National de la Recherche Scientifique, 13 quai Anatole-France, 444 p.
- Katz, H.R., 1963. Revision of Cretaceous stratigraphy in Patagonian cordillera of Ultima Esperanza, Magallanes province, Chile. *American Association of Petroleum Geologists Bulletin* 47 (3), 506–524.
- Katz, H.R., 1972. Plate tectonics and orogenic belts in the southeast Pacific. *Journal of the Royal Society New Zealand* 237 (5354), 331–332.
- Klepeis, K.A., 1994. Relationship between uplift of the metamorphic core of the southernmost Andes and shortening in the Magallanes foreland fold and thrust belt, Tierra del Fuego, Chile. *Tectonics* 13 (4), 882–904.
- Klepeis, K.A., Austin, J.M., 1997. Contrasting styles of superposed deformation in the southernmost Andes. *Tectonics* 16 (5), 755–776.
- Kohn, M.J., Spear, F.S., Harrison, T.M., Dalziel, I.W.D., 1995. $^{40}\text{Ar}/^{39}\text{Ar}$ geochronology and P - T - t paths from the Cordillera Darwin metamorphic complex, Tierra del Fuego, Chile. *Journal of Metamorphic Geology* 13, 251–270.
- Kraemer, P.E., 1991. Estructura y Evolución de los Andes Patagónicos entre los 49°40' y 50°40' Latitud Sur. Provincia de Santa Cruz, Argentina, Universidad Nacional de Córdoba.
- Kraemer, P.E., 1996. Regional balanced cross-section in the Patagonian Andes of Tierra del Fuego (Argentina and Chile). *Troisieme Symposium International sur la Geodynamique Andine*, Resumes Etendus, pp. 407–410.
- Kraemer, P.E., 1998. Structure of the Patagonian Andes. Regional balanced cross section at 50° S.L. Argentina. *International Geology Review* 40, 896–915.

- Kraemer, P.E., Introcaso, A., Robles, A., 1996. Perfil geológico-gravimétrico regional a los 50° latitud sur. Estructura crustal y acortamiento andino. Cuenca Austral y Cordillera Patagónica. 14th Congreso Geológico Argentino y 4th Congreso de Exploración de Hidrocarburos 2, 423–432.
- Macellari, C.E., Barrio, C.A., Manassero, M., 1989. Upper Cretaceous to Paleocene depositional sequences and sandstone petrography of southwest Patagonia (Argentina and Chile). *Journal of South American Earth Sciences* 2 (3), 223–239.
- Malumian, N., Nañez, C.A., 1988. Asociaciones de foraminíferos del Terciario medio de Cuenca Austral: sus relaciones con eventos eustáticos globales. *Revista de la Asociación Geológica Argentina* 43 (2), 257–264.
- Mingramm, A.R.G., 1982. Evolution Scheme of fuegian Andes along Los Cerros-Pla Hardy Section, Shell, Holanda.
- Natland, M.L., Gonzalez, E., Cañon, A., Ernst, M., 1974. A system of stages for correlation of Magallanes basin sediments, p. 126.
- Nelson, E.P., 1982. Post-tectonic uplift of the Cordillera Darwin orogenic core complex: evidence from fission track geochronology and closing temperature–time relationship. *Journal of the Geological Society of London* 130, 755–762.
- Nelson, E.P., Dalziel, I.W.D., Milnes, A.G., 1980. Structural geology of the Cordillera Darwin-collision style orogenesis in the southernmost Andes. *Eclogae Geologicae Helveticae* 73, 727–751.
- Nelson, E.P., Bruce, B., Elthon, D., Weaver, S., 1988. Regional lithologic variations in the Patagonian batholith. *Journal of South American Earth Sciences* 1, 239–247.
- Olivero, E.B., Malumian, N., 1999. Eocene stratigraphy of southeastern Tierra del Fuego island, Argentina. *American Association of Petroleum Geologists Bulletin* 83 (2), 295–313.
- Ramos, V.A., 1979. Tectonica de la región del Río y Lago Belgrano, Cordillera Patagónica, Argentina. 2nd Congreso Geológica Chileno IB, 1–32.
- Ramos, V.A., 1989. La faja plegada y corrida de la Cordillera Patagonica Austral, Provincia de Santa Cruz, Argentina. 1st Congreso Nacional de Exploración de Hidrocarburos 2, 951–970.
- Ramos, V.A., Niemeyer, H., Skarmeta, J., Muñoz, J., 1982. Magmatic evolution of the Austral Patagonian Andes. *Earth and Planetary Science Letters* 18, 411–442.
- Rapalini, A.E., Hervé, F., Ramos, V., Singer, S., 2001. Paleomagnetic evidence for a very large counterclockwise rotation of the Madre de dios archipiélago, southern Chile. *Earth and Planetary Science* 184 (2), 471–487.
- Riccardi, A.C., Rolleri, E.O., 1980. Cordillera Patagónica Austral. 2nd Simposio de Geología Regional Argentina 1 (2), 1173–1306.
- Russo, A., Flores, M.A., Di Benedetto, H., 1980. Patagonia Austral extrandina. 2nd Simposio de Geología Regional Argentina 2, 1431–1462.
- Saunders, A.D., Tarney, J., Stern, C., Dalziel, I.W.D., 1979. Geochemistry of Mesozoic marginal basin floor igneous rocks from southern Chile. *Geological Society of America Bulletin* 90 (3), 1237–1258.
- Scott, K.M., 1966. Sedimentology and dispersal pattern of a Cretaceous flysh sequence, Patagonian Andes, southern Chile. *American Association of Petroleum Geologists Bulletin* 50 (1), 72–107.
- Stern, C.R., Elthon, D., 1979. Vertical variation in the effects of hydrothermal metamorphism in Chilean ophiolites; their implications for ocean floor metamorphism. *Tectonophysics* 55 (1–2), 179–313.
- Stern, C.R., Mukasa, S.B., Fuenzalida, R., 1991. Age of the Sarmiento ophiolite complex and the Rocas Verdes marginal basin, Magallanes, Chile. 6th Congreso Geológica Chileno, Resúmenes Ampliados, 241–243.
- Suarez, M., 1979. Late Mesozoic island arc in the Southern Andes, Chile. *Geological Magazine* 116 (3), 181–190.
- Suarez, M., Pettigrew, T.H., 1976. An upper Mesozoic island-arc-backarc system in the southern Andes and South Georgia. *Geological Magazine* 113, 305–328.
- Suarez, M., Herve, M., Puig, A., 1985. Hoja Isla Hoste e islas adyacentes. Servicio Nacional de Geología y Minería de Chile, 133.
- Suppe, J., 1983. Geometry and kinematics of fault bend folding. *American Journal of Science* 283, 684–721.
- Suppe, J., Medwedeff, D.A., 1990. Geometry and kinematics of fault-propagation folding. *Eclogae Geologicae Helveticae* 83 (3), 409–454.
- Thomas, C.R., 1949. Geology and petroleum exploration in Magallanes province, Chile. *American Association of Petroleum Geologists Bulletin* 33 (9), 1553–1578.
- Uliana, M.A., Biddle, K.T., Phelps, D.W., Gust, D.A., 1985. Significado del vulcanismo y extensión mesojurásicos en el extremo meridional de Sudamérica. *Revista de la Asociación Geológica Argentina* 36 (3–4), 63–97.
- Wilson, T.J., 1991. Transition from back-arc to foreland basin development in the southernmost Andes: stratigraphic record from Ultima Esperanza District, Chile. *Geological Society of America Bulletin* 103, 98–111.
- Winn, R.D., 1978. Upper Mesozoic flysh of Tierra del Fuego and South Georgia Island: a sedimentological approach to lithosphere plate restoration. *Geological Society of America Bulletin* 89 (4), 533–547.
- Winslow, M.A., 1981. Mechanisms for basement shortening in the Andean foreland fold belt of southern South America. In: McClay, K.R., Price, N.J. (Eds.), *Thrust and Nappe Tectonics*, Geological Society of London by Blackwell Scientific Publications, pp. 513–528.
- Winslow, M.A., 1982. The structural evolution of the Magallanes Basin and Neotectonics in the Southernmost Andes. In: Craddock, C., (Ed.), *Antarctic Geoscience*, University of Wisconsin, Madison, pp. 143–154.
- Yañez, G.A., Vera, E., Parra, J.C., 1988. Basement structures in the southern part of the Magallanes basin, Chile: a geographical approach. 6th Congreso Geológica Chileno, Resúmenes Ampliados, pp. 64–67.